Silicon (2024) 16:4461–4470
https://doi.org/10.1007/s12633-024-03003-x

RESEARCH

Crystallization of Hydrogenated Amorphous Silicon Thin Films Using Combined Continuous Wave Laser and Thermal Annealing

Adnan Shariah[1]

Received: 19 January 2023 / Accepted: 22 April 2024 / Published online: 11 May 2024

Abstract

The thermal process of amorphous silicon thin film crystallization when combined with an aluminum (Al) film using a continuous wave (CW) laser is accompanied by additional interactions induced by the aluminum layer. This technique is frequently employed to optimize the crystallization process and enhance the quality of crystalline silicon by combining the thermodynamic effects of laser annealing with metal-induced crystallization (MIC). Hydrogenated amorphous silicon (a-Si:H) films were deposited using the plasma-enhanced chemical vapor deposition (PECVD) process on Corning glass substrates. An aluminum overcoat was deposited on the films. The specimens were irradiated with a continuous wave (CW) argon-ion (Ar +) laser beam of varying power density and duration. The samples were then annealed at 250 °C for 15 min to convert the amorphous silicon into polysilicon film. The grain size of the polycrystalline silicon films varies by varying the laser power density and the exposure time. The polysilicon grains acquired diameters ranging from 0.4 to 1.25 µm when the laser power density was set between 74.7 W/cm^2 and 94.3 W/cm^2. The grains with a size ranging between 1 and 2.5 µm showed plate-like and dendritic-like configurations when laser power densities changed between 31.4 and 74.7 W/cm^2. The X-ray diffraction analysis (XRD) analysis revealed polycrystalline silicon with expected relative strengths.

Keywords Laser and thermal assisted crystallization · Metal-induced crystallization · Low-temperature crystallization · Polysilicon solar cells · Crystallization of amorphous silicon

1 Introduction

Polycrystalline silicon (Poly-Si) is a critical component of the semiconductor industry's manufacturing process. It has widespread application in various electrical devices, including solar cells and thin film transistors (TFTs) [1–4]. Solar cell devices made of polycrystalline silicon thin films of a few micrometers in grain are expected to have adequate optical and electrical characteristics with the most efficient and least expensive combination. Solar cells with high efficiency are made of highly costly single-crystalline silicon, while low-cost solar cells are made of amorphous silicon but have low efficiency. The constraints of hydrogenated amorphous silicon (a-Si:H), such as low carrier mobility [5] and instability due to applied bias, temperature, and light exposure [6, 7], do not appear in the use of Poly-Si in solar cells.

Poly-Si thin films can be obtained by a variety of chemical vapor deposition processes, which include low-pressure chemical vapor deposition (LPCVD) [8], atmospheric pressure chemical deposition (APCVD) [9], and plasma-enhanced chemical vapor deposition (PECVD) [10]. In all these processes, there is a transition temperature (greater than 600 °C) above which the resultant as-deposited film is polycrystalline [11]. This processing temperature is too high (for large areas of glass or plastic substrates), limiting the use of low-cost substrates such as glass and plastic. The challenge is fabricating Poly-Si thin films on such substrates at low temperatures. Although it is possible to use certain types of crystallization at low temperatures to form Poly-Si films of reasonable large grain size, Poly-Si films produced by the crystallization of a-Si:H has far superior material and electronic properties than as-deposited Poly-Si due to the larger grains [12, 13], higher conductivity [13], larger breakdown voltages of metal–oxide–semiconductor capacitance

The author did not receive support from any organization for the submitted work.

✉ Adnan Shariah
shariah@just.edu.jo

[1] Department of Applied Physics, Jordan University of Science and Technology, Irbid 22110, Jordan

[14], and adequate mobility that are over 100 times larger than a-Si [15, 16]. However, it has been demonstrated that the crystallization temperature of a-Si:H can be significantly reduced in metal films [17–19]. Annealing of a-Si:H films by laser is another technique used to produce large-grain-sized Poly-Si films [3, 4, 20–28]. This technique is usually used for making thin film transistors (TFTs) on low-cost substrates. The diameter of the laser beam spot used in the literature is minimal, about 100 mm for CW laser and about 10 mm for pulsed laser [26–28]. However, because of the small size of the spot, this technique cannot be used to crystallize large a-Si:H films, which are required for Poly-Si solar cells. The researchers, Volkovaynova et al. [29], investigated the consequences of subjecting amorphous silicon films (1 µm in thickness) which are in contact with aluminum thin films (0.3 µm in thickness) using a pulsed laser with a beam diameter of 20 µm and a pulse power ranging from 0.2 to 0.6 W. The authors termed this process "laser-assisted metal-induced crystallization." They hypothesized that aluminum film would absorb the energy of laser pulses and cause it to evaporate. Upon complete evaporation of the Al film, thermal energy transfer begins to the a-Si film. When the scanning rate was 250 mm/s and the laser power was 0.2 W, their findings indicated that aluminum evaporation was incomplete and that a-Si films did not crystallize. However, when employing reduced scanning rates and/or higher laser power, the a-Si films undergo a crystallization process. The aforementioned findings are shown through Raman spectroscopy.

Our aim in the present work is to use a CW laser beam of low power density to generate nuclei of crystals in the a-Si:H films that are in contact with the aluminum layer. The films will then be crystallized with aluminum assistance in a furnace at low temperatures in a relatively short time. In this process, the a-Si:H film is concentrated in two steps: laser-assisted metal-induced nucleation followed by thermal annealing.

2 Experimental Technique

Corning 7059 glass plates were used as substrates for a-Si:H film deposition. The glass substrates were cleaned using Trichloroethylene (TCE), acetone, and methanol in an ultrasonic bath. Intrinsic a-Si:H films were deposited on the substrate using PECVD system. During the deposition, the temperature, pressure, silane flow rate, and radio-frequency power were kept at 250 °C, 0.5 torr, 20 sccm, and 3 W, respectively. A 380 nm intrinsic a-Si:H film was deposited on top of the glass at 11.5 nm per minute. After deposition, the samples were allowed to cool to room temperature in a vacuum to prevent oxidization. The chamber was then filled with nitrogen to atmospheric pressure.

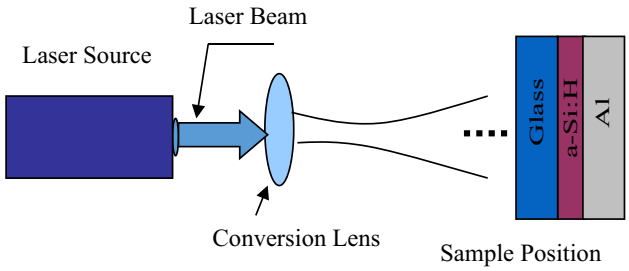

Fig. 1 Schematic diagram of the arrangement used in laser treatment

The samples were immediately transferred to a thermal evaporation system where an Al film was evaporated on the a-Si:H layer under a pressure of 1.2×10^{-6} mbar at room temperature using the evaporative coating system. The deposition rate was kept at 0.8 nm/sec, and the Al film thickness was about 300 nm. The samples were then irradiated by a CW laser beam of power densities ranging from 31.4 W/cm^2 to 94.3 W/cm^2 for irradiation times ranging from 5 to 600 s. The wavelength of the utilized laser beam is 514.5 nm. The samples are irradiated from the glass side (front side), and light that is not absorbed by the a-Si:H film in the first pass is reflected by the aluminum film on the back side. The laser's power density was reduced using a converging lens to examine the influence of the laser's power density on the crystallization process. As the beam extends beyond the focus point, spots

Table 1 Laser power density, laser spot diameter and area, and exposing duration used

Laser Power (W)	Laser Power Density (W/cm^2)	Laser Spot Diameter (mm)	Laser Spot Area (mm^2)	Exposing Time to Laser (sec)
2.4	94.3	1.8	2.5	5 10 15 60
4.8	87	2.65	5.5	10 60 300
1.9	74.7	1.8	2.5	5 10 60 300
1.5	59	1.8	2.5	300
5.8	33.3	4.7	17.4	75 150 300 600
0.8	31.4	1.8	3.1	10 60 300

Only thermal annealing process (no laser) 15 min

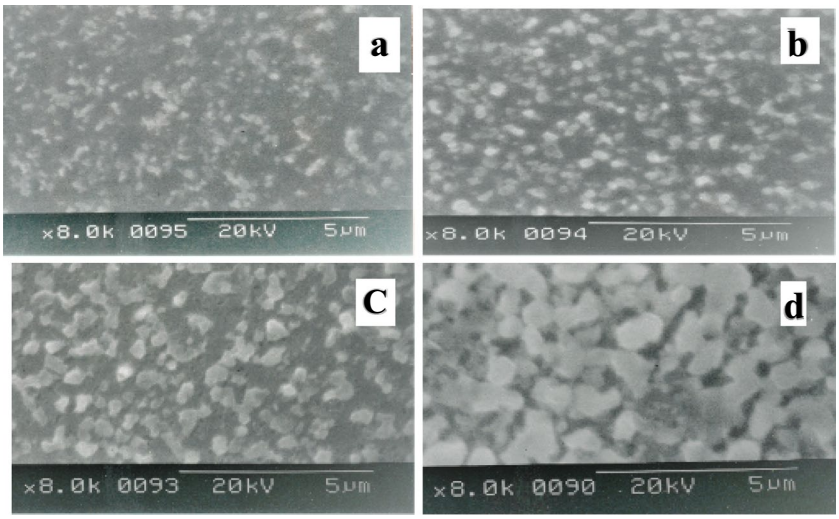

Fig. 2 SEM photographs of a-Si:H thin films irradiated by CW laser of power density 94.3 W/cm^2 for different time durations; **a**) 5 s, **b**) 10 s, **c**) 15 s, **d**) 60 s. Thermally annealed at 250 °C for 15 min

of varying sizes may form at various distances from the focal point. By positioning the sample in different positions, small or large sample portions can be exposed to the laser. The purpose of a lens is to change the laser power density while producing a wide laser beam. This is desirable because larger areas could be scanned faster if the film could be converted to Poly-Si in the first step of the present crystallization process. This would allow using a continuous-wave laser source to generate large-sized thin films to fabricate low-cost solar cells. Figure 1 shows the arrangement used during laser treatment.

Finally, the samples were thermally annealed in a nitrogen environment at 250 °C for 15 min. The a-Si:H film is presumably to be converted to Poly-Si after this treatment, and it was examined using the XRD technique before the aluminum (Al) film was etched out. The Al film was removed by a standard etching solution (85 parts phosphoric acid, 5 parts nitric acid, 5 parts acetic acid, and 5 parts deionized water) at 50 °C.

Optical and scanning electron microscopes (SEM) were used to investigate the surface morphology. XRD measurements were performed on the a-Si:H films using a Philips model X'Pert x-ray diffractometer. Under the thin-film optics configuration, the 2θ scan was performed at a shallow fixed setting of 2.5 degrees.

3 Results and Discussion

Table 1 summarizes the laser power densities, spot diameters, spot areas, and irradiation times used in this work.

3.1 SEM Study

Figure 2 is a SEM image depicting the surface morphology of samples irradiated by an Ar-ion laser with a power density of 94.3 W/cm^2 for varying time durations, followed by annealing with Al on top of the a-Si: H layer under the aforementioned conditions. Clearly, crystallization occurred under these circumstances. The size of the Poly-Si grains is highly dependent on the laser beam's irradiation period. Figure 2a depicts a sample that was laser-irradiated for 5 s. The Poly-Si grains are very small, even when the exposer time is 10 s, Fig. 2b. When the irradiation period is increased to 15 s, the grains become larger, Fig. 2c. When exposer time is 60 s the grains size is between 1.0 and 1.2 µm in diameter and cover approximately 90% of the surface, Fig. 2d.

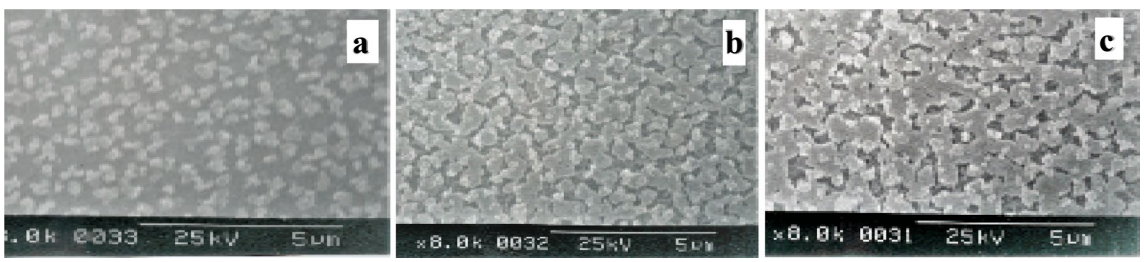

Fig. 3 SEM photographs of a-Si:H thin films irradiated by CW laser of power density of 87 W/cm^2 for different time durations; a) 10 s, b) 60 s, c) 300 s. Thermally annealed at 250 °C for 15 min

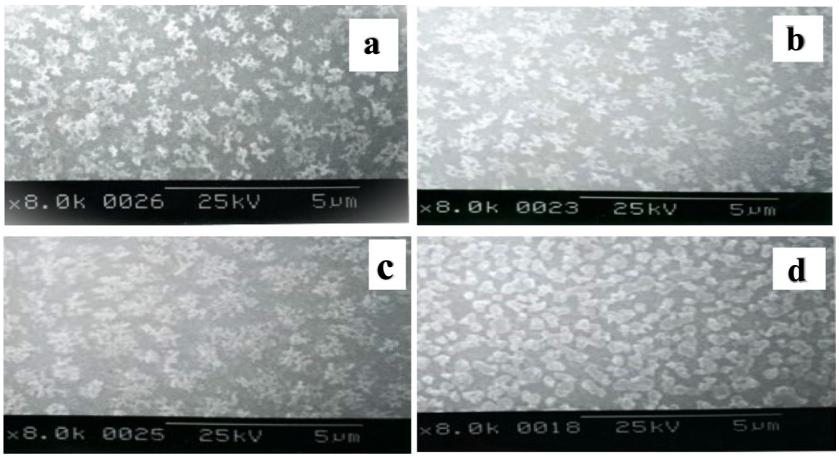

Fig. 4 SEM photographs of a-Si:H thin films irradiated by cw-Ar^+ laser of power density of 74.7 W/m^2 for; **a**) 5 s, **b**) 10 s, **c**) 60 s, **d**) 300 s. Thermally annealed at 250 °C for 15 min

When samples are placed 29.4 cm from the lens's focal point, the laser spot size is measured to be 2.65 µm, and the laser power density on the samples is calculated to be 87 W/cm^2. The samples were exposed to this power density for three periods of 10 s, 60 s, and 300 s, then thermally annealed at 250°C for 15 min.

Figure 3 illustrates the SEM images of these samples. These images show that after 10 s of exposure to the laser beam, the a-Si:H film is converted to Poly-Si having small grains (Fig. 3a). When exposer time is 60 s the grains are considerably larger and almost entirely cover the surface, Fig. 3b. The sample irradiated by laser for 300 s, (Fig. 3c), grains in this sample are almost identical to those in the 60-s film. This demonstrates that the film has crystallized entirely after 60 s of laser exposure.

When samples irradiated by laser of density 94.3 W/cm^2 and 87 W/cm^2 for the same durations, 10 s and 60 s, respectively. It is observed that samples irradiated for 10 s has the same grain size and about the same density, while grains in sample irradiated for 60 s by laser of density 94.3 W/cm^2 are larger than those irradiated laser of density 87 W/cm^2. This demonstrates that irradiation duration affects the crystallization process.

Another set of samples was exposed to a lower power density laser beam at 74.7 W/cm^2. As illustrated in Fig. 4, the SEM images of these samples reveal a variety of different morphologies. Many plate-like crystals develop in these samples, with a dendrite-like morphology that varies in width depending on the exposure time to the laser beam. The crystallite size is approximately 0.8 µm when the period is 5 s, and the coating covers nearly 50% of the film area, Fig. 4a. Increasing the exposure duration to 10 s resulted in larger plate-like crystallites of approximately 1 µm, Fig. 4b. The surface morphology of a sample subjected to the same laser beam for 60 s is shown in Fig. 4c. The crystallites are more extensive and denser, covering approximately 75% of the film surface. Another sample was examined after being subjected to the laser beam for 300 s (Fig. 4d). It illustrates various crystal types compared to films treated by a laser beam of the same power density (Fig. 4a–c). The crystallites are approximately 1.6 µm in diameter and cover about 80% of the surface. When compared to grains made by a laser beam with a higher power density, these grains are about the same size and density as those made by a laser beam with 87 W/cm^2 when the film was exposed for 10 s.

Another sample was exposed for 300 s to a laser beam with a lower power density, 59 W/cm^2, as shown in Fig. 5. The picture shows the formation of dendrite-type Poly-Si crystallites of size 2 µm, covering around 80% of the surface. These grains are larger than those produced by higher power density but shorter exposure time laser beams (Fig. 4a–c).

The SEM micrographs of the samples treated with laser beams of 33.3 W/cm^2 power density and irradiated with periods of 75 s, 150 s, 300 s, and 600 s are shown in Fig. 6.

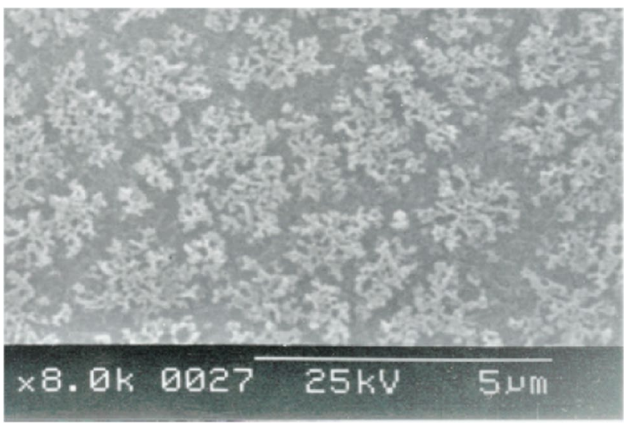

Fig. 5 SEM photographs of a-Si:H thin film irradiated by CW laser of power density of 59 W/cm^2 for 300 s. Thermally annealed at 250 °C for 15 min

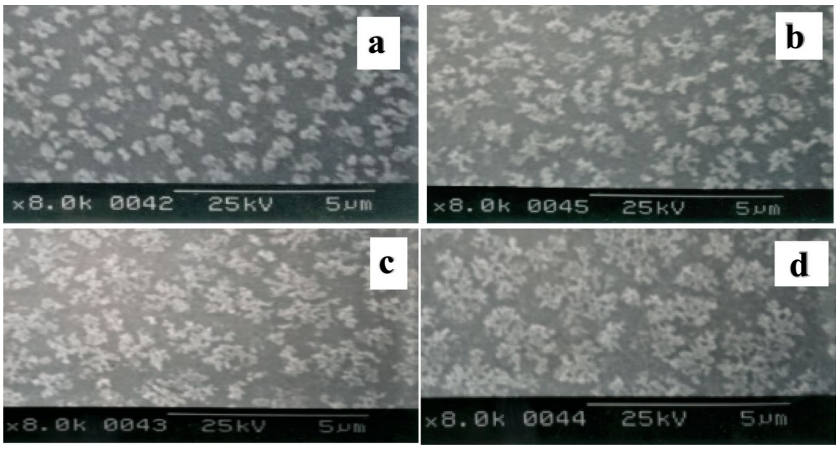

Fig. 6 SEM photos of a-Si:H thin films irradiated by cw-Ar^+ laser of power density of 33.3 W/cm^2 for different time; **a**) 75 s, **b**) 150 s, **c**) 300 s, **d**) 600 s. Thermally annealed at 250 °C for 15 min

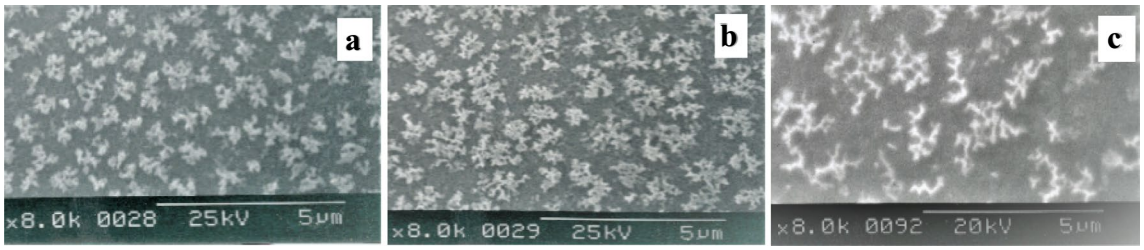

Fig. 7 SEM photographs of a-Si:H thin films irradiated by cw-Ar^+ laser of power density of 31.4 W/cm^2 for different time; **a**) 10 s, **b**) 60 s, **c**) 300 s. Thermally annealed at 250 °C for 15 min

Film has Poly-Si crystals that look like dendrites and change in patterns, size, and shape depending on how long they are exposed to light. More extensive and denser crystals are formed when films are exposed to a laser beam for an extended period.

Compared to images obtained with a higher power density laser (Figs. 2, 3, and 4), it is clear that Fig. 6d is very similar to Fig. 5, where the laser's power density was 33.3 W/cm^2 and 59 W/cm^2, respectively, but the exposure period was 600 s and 300 s, respectively. It is obvious that when the laser power density is reduced, the exposure time required to achieve the same film structure in terms of crystal pattern, size, and density must be increased. Furthermore, significant similarities appear between Fig. 6c (33.3 W/cm^2 for 300 s) and Fig. 4c (74.7 W/cm^2 for 60 s), as well as between Fig. 6b (33.3 W/cm^2 for 150 s) and Fig. 4b (74.7 W/cm^2 for 10 s).

Another group of samples was subjected for 10 s, 60 s, and 300 s to a laser beam with a power density of 31.4 W/cm^2. Figure 7 illustrates the surface morphology of these materials. Dendrite-type crystals of around 0.7 μm in size are created in the films after 10 s of laser exposure (Fig. 7a). However, the crystals of about 2 μm appeared after 60 s of laser exposure (Fig. 7b). The crystallites in samples exposed for 300 s (Fig. 7c) are different from those exposed for 10 and 60 s. Here the crystallites are larger but less dense in this case, reaching a length of up to 3.9 μm. Finally, without a laser, one sample was thermally annealed (at 250 °C for 15 min).

Figure 8 shows the SEM image, which reveals the formation of dendrite-type crystals with a size of 1.4 μm in the film. When compared to the images of samples treated with a laser before thermal annealing, it is clear that the morphology of the sample's surface morphology is similar to several of them. This indicates that the crystallization process in

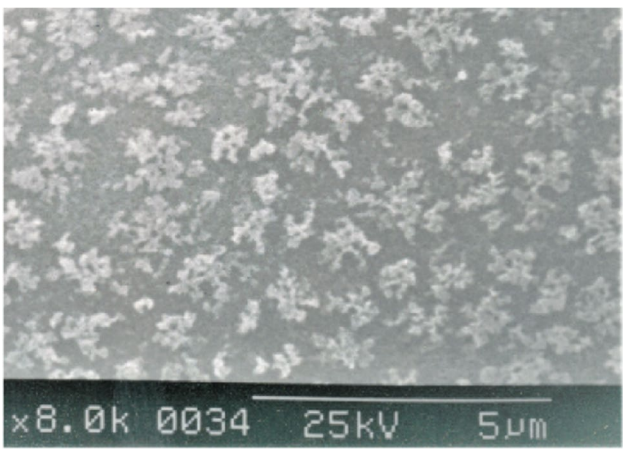

Fig. 8 SEM photographs of a-Si:H thin films thermally annealed at 250 °C for 15 min. No laser irradiation was used

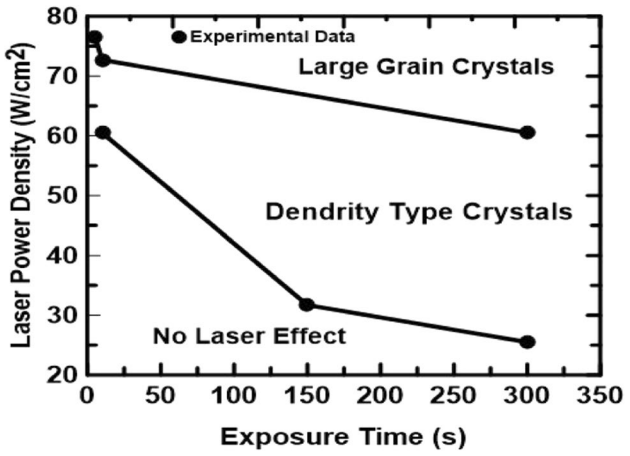

Fig. 9 Effect of laser power density and exposure time on the nature of crystals produced and approximate boundaries for laser power produce a specific type of crystallization

these materials is primarily due to metal-induced thermal annealing, with little influence from laser treatment.

The data reported in Figs. 2, 3, 4, 5, 6, 7 and 8 illustrates that crystallization requires a minimum power density (threshold value) and a minimum exposure time. At high laser power densities and longer exposure times, two distinct forms of Poly-Si crystallites form in the films: large grains and dendrite-like crystals. When the laser intensity and exposure time are less than a specific value, crystallization occurs only due to metal-induced thermal annealing, with no influence from the laser in this domain. The three areas' border lines are depicted in Fig. 9. These findings provide insight into the crystallization technique employed in this work, including laser-assisted and metal-induced heat crystallization.

Based on the results of this study, we proposed the following crystallization mechanism for the utilized technique: When an amorphous silicon film in contact with an aluminum film is exposed to a laser, the activation energy of aluminum and silicon atoms inside the treated volume increases as well. As the material absorbs the laser energy, it is transformed into heat. The added heat heats the exposed region of the film, causing its temperature to rise to a value dependent on the laser beam's power density. When the power density is high enough, between 87 W/cm^2 and 94.3 W/cm^2, aluminum atoms diffuse into the amorphous silicon layer, forcing the silicon atoms to organize into grains or clusters of polysilicon rich in aluminum atoms. These grains or clusters continue to grow as the sample is continually subjected to the laser. As seen in Figs. 2 and 3, the size of these grains depends on the laser power and exposure time. When their sizes are less than the thickness of the amorphous film, the growth occurs in three dimensions; otherwise, the growth would have happened in two dimensions. Fewer aluminum atoms diffuse into the amorphous silicon area when the power density is less than 87 W/cm^2, forming nucleation sites. This amount of aluminum is limited to forcing the silicon atoms to rearrange themselves in preferable directions to form dendritic type clusters of polysilicon. This concept, we feel, is consistent with the data found in other studies.

Note that the absolute values shown in Fig. 9 only apply to the current layer stack and deposition method using a-Si:H. As the crystallization process involves the movement of atoms within the amorphous structure to form a more ordered lattice, amorphous substances are transformed into crystals. The activation energy barrier must be overcome for this transformation to take place. Consequently, the quantity of energy required for the atoms to begin rearranging themselves may vary based on the layers' thicknesses and stake, and film preparation method. For example, Shariah and Bataineh [30] have showed that Crystallization of PECVD-prepared a-Si:H films occurred at an annealing temperature of 250 °C, even after only 15 min., whereas, Crystallization of sputtered a-Si on glass substrates starts at 300 °C and when annealed for at least135 minutes. This duration is needed even if it is annealed at higher temperatures (350 °C).

Nast and Hartmann [31] studied the Al oxide interface layer effect between Al and Si films on the crystallization process during aluminum-induced amorphous silicon crystallization. The aluminum oxide layer forms naturally after 48 h of exposure to air. The samples were annealed

Table 2 Power density and exposure time values are used in the present work, together with those used by other researchers

	Laser Power Density (W/cm^2)	Exposure Time (s)	Film Type	Film Thickness (nm)
Present work	31.4 – 94.3	5—600	Al/a-Si: H/Glass	380
Ref [20]	12.5×10^6	0.002	a-Si/alkaline/glass	50–150
Ref [21]	25×10^3	0.001	a-Si:H/Glass	50—500
Ref [22]	30×10^3	0.004	a-Si:H/Glass	360
Ref [23]	$0.01–20\times10^3$	5	a-Si:H/Quartz	500
Ref [25]	High power	Until melting	a-Si:H/glass	300
Ref [26]	No information	No information	a-Si:H/Glass	1000–2000
Ref. [29]	Laser power (0.2 -0.6) W	Scanning rate (25–250) mm/s	a-Si/Glass	1000

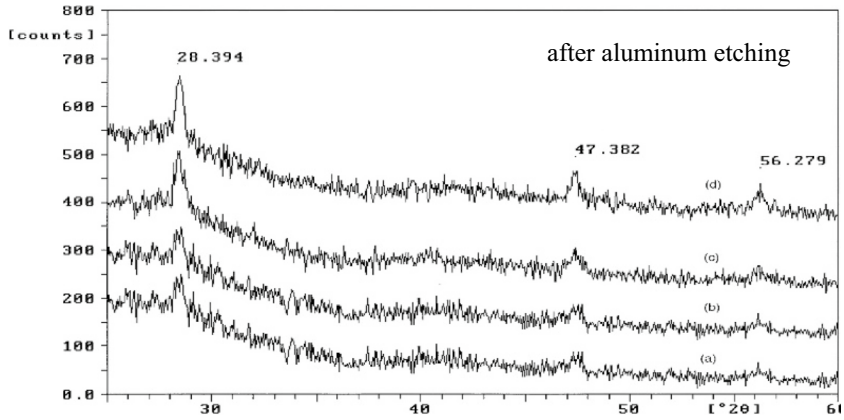

Fig. 10 XRD measurements of a-Si:H thin films exposed to laser power density of 87 W/cm^2 for exposure times; **a**) no laser, **b**) 10 s, **c**) 60 s and **d**) 300 s

for 30 min at 475 °C. They observed that the aluminum oxide layer limits the nucleation and enables silicon star-like grains to grow to enormous sizes. A thinner Al oxide layer, on the other hand, resulted in a silicon system formed of a large number of tiny silicon grains. Nast and Hartmann [31] observed star-like grains that resemble those produced by low-power lasers, as shown in Figs. 4, 5, 6, 7 and 8. These findings support our hypothesis that the amount of aluminum diffused into the amorphous silicon region significantly influences the size, shape, and number of poly-silicon grains produced by laser-induced and metal-assisted crystallization.

The most remarkable result of this work is that the laser's power density is significantly less than that used by other researchers [20, 21, 23–25]. The maximum laser power density used in this research was about 94.3 W/cm^2 for 5 to 300 s. In contrast, other studies have used power densities ranging from approximately (8 to 560 kW/cm^2) for exposure durations ranging from (0.72 ms to 2 ms) [20, 21, 23, 25, 27–29] and (0 to 200 min) [24]. Table 2 compares the power densities and exposure times utilized in this study to those employed by other studies.

3.2 XRD Study

Additionally, we investigated the samples using X-ray diffraction to determine the change in the structure of the a-Si:H film. The XRD scan of amorphous silicon exhibits no peak.

However, when crystallized samples are examined using an XRD, peaks arise, indicating the formation of Poly-Si inside the amorphous silicon. This approach may compute many parameters, including the crystalline volume percentage, grain size, orientation, film thickness, and film quality. Figures 10, 11, 12 and 13 show the XRD scans of samples subjected to lasers with power densities of 87 W/cm^2 and 33.3 W/cm^2 for varying exposure durations. Figure 10 shows samples that have been irradiated with a laser power density of 87 W/cm^2 for various periods before annealing. This figure indicates that when there is no laser treatment or when laser exposure duration is ten seconds, there are no peaks at angles associated with the presence of Poly-Si. A comparison is made between the results obtained from SEM and XRD for a single sample that was irradiated with a laser of power (87 W/m2 for 300 s). The XRD curve indicates that the average particle size is approximately 20 nm, whereas the SEM image

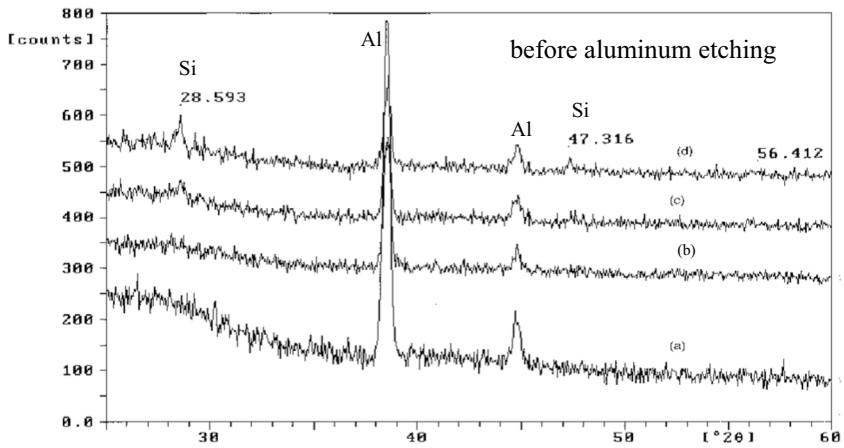

Fig. 11 XRD measurements of a-Si:H thin films exposed to laser power density of 87 W/cm^2 for exposure times; **a**) no laser, **b**) 10 s, **c**) 60 s and **d**) 300 s

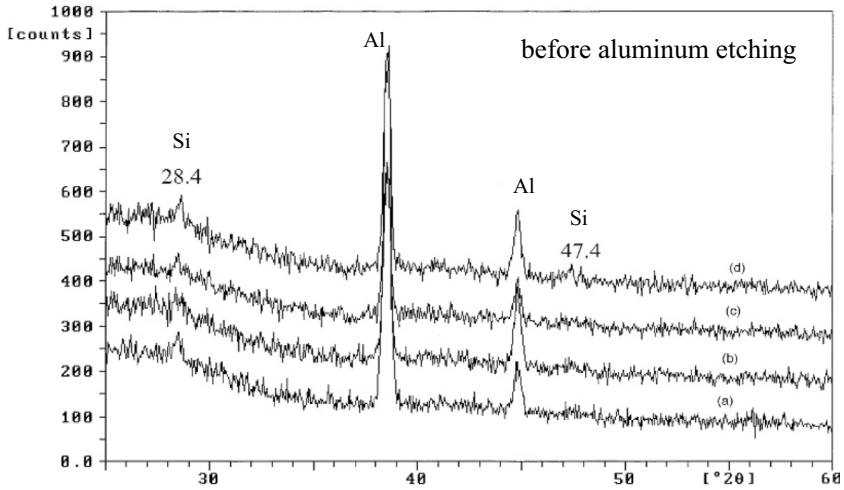

Fig. 12 XRD measurements of a-Si:H thin films exposed to laser of power density of 33.3 W/cm^2 for exposure times; **a**) 75 s, **b**) 150 s, **c**) 300 s, **d**) 600 s

indicates approximately 70 nm. On the other hand, when samples are laser irradiated for 60 or 300 s, there are peaks at relative angles. However, after annealing the samples at 250 °C for 15 min and etching the aluminum, the XRD scan, Fig. 11, reveals three peaks at 28.5, 47.4, and 56.3 degrees. These are signs that Poly-Si is there, and they clearly show that a Poly-Si film has formed in the a-Si film. Peaks at about 38.5° and 45° belongs to aluminum.

XRD observations of samples subjected to a laser power density of 33.3 W/cm^2 for various periods before annealing are shown in Fig. 12. Relatively small peaks were detected at 2θ values of 28.5 degrees.

On the other hand, after annealing the samples, the Poly-Si spectra are shown in Fig. 13, together with their expected relative intensities. The figure reveals three peaks at 28.5, 47.4, and 56.3 degrees, mainly caused by thermal annealing.

4 Conclusion

The current study demonstrated using a CW-laser with the lowest power densities in conjunction with aluminum-induced thermal annealing to crystallize a-Si:H films produced on glass substrates by the PECVD process. The findings show that, with the aid of a CW laser, sizable Poly-Si grains could be created in the film at an annealing temperature of 250°C and an annealing period of 15 min. SEM analysis demonstrates that the laser power density and the irradiation duration significantly influence the type and quantity of Poly-Si crystals. Aluminum-induced thermal annealing of samples previously subjected to laser power at relatively low temperature, as revealed by XRD studies, plays a significant role in crystallization. In addition, the results indicate that the crystallization of the a-Si:H film is influenced by the laser power density, exposure time, and thermal annealing.

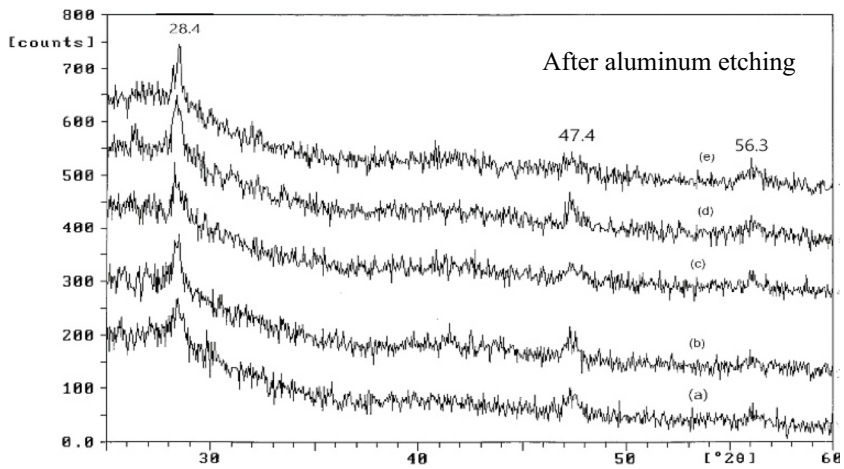

Fig. 13 XRD measurements of a-Si:H thin films exposed to laser of power density of 33.3 W/cm^2 for exposure times; **a**) 75 s, **b**) 150 s, **c**) 300 s, **d**) 600 s, **e**) 0 s

Further investigation is necessary to determine the most effective values for each parameter in the presence of varying annealing temperatures and times. Ultimately, this research introduces the interesting prospect of making Poly-Si from a-Si:H using an extremely low-power laser with the aim of manufacturing large-area Poly-Si solar cells, as laser spots can be enlarged to a reasonable size.

Acknowledgements The author would like to thank Prof. Hameed Naseem of Arkansas University's electrical engineering department for sample preparation and Prof. Surendra Singh of the Physics department for enabling me to utilize his laser facility.

Author contributions AS carried out the experimental work, AS put shape for the research, AS analyzed and interpreted the results, AS prepared the figures, AS wrote the final version and reviewed the manuscript.

Data Availability The data that support the findings of this study are available from the corresponding author, [AS], upon reasonable request**.**

Declarations

Ethics Approval Not applicable.

Consent to Participate Not applicable.

Consent for Publication Not applicable.

Competing interests The authors declare no competing interests.

References

1. Park M et al (2020) Comprehensive analysis of blue diode laser-annealing of amorphous silicon films. Thin Solid Films 696:137779
2. Çınar K, Yesil C, Bek A (2019) Revealing laser crystallization mechanism of silicon thin films via pulsed IR lasers. J Phys Chem C 124(1):976–985
3. Do Y et al (2020) Remarkable improvement in foldability of poly-Si thin-film transistor on polyimide substrate using blue laser crystallization of amorphous Si and comparison with conventional poly-Si thin-film transistor used for foldable displays. Adv Eng Mater 22(5):1901430
4. Zhang B et al (2007) Polysilicon thin film-transistors with uniform and reliable performance using solution-based metal-induced crystallization. IEEE Trans Electron Devices 54(5):1244–1248
5. Lee S et al (2015) Localized tail states and electron mobility in amorphous ZnON thin film transistors. Sci Rep 5(1):1–9
6. Lai M-H, Wu YCS, Chang C-P (2011) Electrical performance and thermal stability of MIC poly-Si TFTs improved using drive-in nickel induced crystallization. Mater Chem Phys 126(1–2):69–72
7. Cattin J et al (2021) Influence of light soaking on silicon heterojunction solar cells with various architectures. IEEE J Photovolt 11(3):575–583
8. Li S et al (2019) In situ-doped silicon thin films for passivating contacts by hot-wire chemical vapor deposition with a high deposition rate of 42 nm/min. ACS Appl Mater Interfaces 11(33):30493–30499
9. He R et al (2016) High pressure chemical vapor deposition of hydrogenated amorphous silicon films and solar cells. Adv Mater 28(28):5939–5942
10. Moreno M et al (2021) Comparative study on the quality of microcrystalline and epitaxial silicon films produced by pecvd using identical sif4 based process conditions. Materials 14(22):6947
11. Sridhar N et al (1996) Effect of deposition temperature on the structural and electrical properties of laser-crystallized hydrogenated amorphous silicon films. J Appl Phys 79(3):1569–1577
12. Chen J et al (2017) Control of grain size and crystallinity of poly-Si films on quartz by Al-induced crystallization. CrystEngComm 19(17):2305–2311
13. Mohiddon M et al (2011) Growth, optical, and electrical properties of silicon films produced by the metal-induced crystallization process. J Nanopart Res 13(11):5999–6004
14. Wu M et al (1999) High electron mobility polycrystalline silicon thin-film transistors on steel foil substrates. Appl Phys Lett 75(15):2244–2246
15. Jang J et al (1998) Electric-field-enhanced crystallization of amorphous silicon. Nature 395(6701):481–483
16. Chan K-Y et al (2008) High-mobility microcrystalline silicon thin-film transistors prepared near the transition to amorphous growth. J Appl Phys 104(5):054506
17. Maity G et al (2019) Aluminum induced crystallization of amorphous Si: Thermal annealing and ion irradiation process. J Non-Cryst Solids 523:119628
18. Hamasha E et al (2016) Aluminum induced crystallization of amorphous silicon thin films with assistance of electric field for solar photovoltaic applications. Sol Energy 127:223–231
19. Pécz B et al (2021) Structural Characteristics of the Si Whiskers Grown by Ni-Metal-Induced-Lateral-Crystallization. Nanomaterials 11(8):1878
20. Hara A et al (2004) High performance low temperature polycrystalline silicon thin film transistors on non-alkaline glass produced using diode pumped solid state continuous wave laser lateral crystallization. Jpn J Appl Phys 43(4R):1269
21. Andrä G et al (2013) Multicrystalline silicon thin film solar cells based on a two-step liquid phase laser crystallization process. 2013 IEEE 39th Photovoltaic Specialists Conference (PVSC), Tampa, FL, USA, pp 1330–1333. https://doi.org/10.1109/PVSC.2013.6744388
22. Said-Bacar Z et al (2012) CW laser induced crystallization of thin amorphous silicon films deposited by EBE and PECVD. Appl Surf Sci 258(23):9359–9365
23. Jin S et al (2016) Lateral grain growth of amorphous silicon films with wide thickness range by blue laser annealing and application to high performance poly-Si TFTs. IEEE Electron Device Lett 37(3):291–294
24. Jia G et al (2014) Nanotechnology enhanced solar cells prepared on laser-crystallized polycrystalline thin films (< 10 μm). Sol Energy Mater Sol Cells 126:62–67
25. Lee Y-J et al (2013) Structural characterization of wavelength-dependent Raman scattering and laser-induced crystallization of silicon thin films. Thin Solid Films 542:388–392
26. Al-Nuaimy E, Marshall J (1996) Excimer laser crystallization and doping of source and drain regions in high quality amorphous silicon thin film transistors. Appl Phys Lett 69(25):3857–3859
27. Farid N et al (2021) Femtosecond laser-induced crystallization of amorphous silicon thin films under a thin molybdenum layer. ACS Appl Mater Interfaces 13(31):37797–37808
28. Chowdhury S et al (2020) Crystallization of Amorphous Silicon via Excimer Laser Annealing and Evaluation of Its Passivation Properties. Energies 13(13):3335
29. Volkovoynova L et al (2022) Heat transfer estimation during laser-assisted metal-induced crystallization of amorphous silicon films.

Proceedings of 8th International Congress on Energy Fluxes and Radiation Effects (EFRE–2022) Tomsk, Russia. https://doi.org/10.56761/EFRE2022.C3-P-005701

30 Shariah A, Bataineh MI (2023) Electrical and Structural Properties of Crystallized Amorphous Silicon Thin Films. Silicon 15(6):2727–2735

31. Nast O, Hartmann AJ (2000) Influence of interface and Al structure on layer exchange during aluminum-induced crystallization of amorphous silicon. J Appl Phys 88(2):716–724